UNIVERSITY OF MICHIGAN
DEPARTMENT OF MECHANICAL ENGINEERING
CAVITATION AND MULTIPHASE FLOW LABORATORY

Report No. UMICH 014571-1-T

INVESTIGATIONS OF SECONDARY LIQUID PHASE STRUCTURE IN STEAM WAKE

(submitted to ASME)

by

S. Krzeczkowski
W. Kim
F. G. Hammitt
J-B. Hwang

Supported by: National Science Foundation Grant
Nos. ENG 75-2315 and GK-40130
and National Academy of Sciences
(with cooperative program with the
Polish Academy of Science)

June, 1976

INTRODUCTION

Wet steam flow has been studied for the break-up of liquid films on flat plates inserted parallel to flow at the trailing edge, as well as liquid droplet stability and disintegration. Some results are shown in this paper.

Moving rotor blading erosion of steam turbine final stages is considered to be still an important problem from the technical and economic point of view. Because of this fact, there is a reason to investigate the liquid phase behavior inside the turbine. In particular, several problems are particularly interesting:

1. condensation of the steam in state downstream of the Wilson line
2. small ($\sim$ 0.05 μm) primary droplets settling upon blades surfaces and liquid film motion due to aerodynamic and centrifugal forces
3. large secondary drop motion and structure
4. erosion of turbine blading and methods useful in avoiding erosion damage

The matter under consideration here concerns the third group of problems. A thin liquid film flowing upon a fixed blade disintegrates at the trailing edge, due to aerodynamic forces. The droplets thus formed are believed to be about four orders of magnitude larger than the primary droplets in the wet steam due to condensation. The maximum droplet size which has been estimated based on theoretical approach (1) for the last stage

of the turbine was around 300 μm, and other authors have expected droplets to be larger than 1 mm (2),(3), using experimental turbines for their research.

The main purpose of the work hereby presented is to measure the relationship between droplet stream structure and the flow conditions. This has been done according to the suggested procedure of J. Kryżanowski (4) in his work at the University of Michigan.

EXPERIMENTAL EQUIPMENT USED

Figure 1 is a schematic representation of our experimental facility and the pertinent flow parameters are as below:

$(p_3)_{max}$ = 3.75 psia = $0.258 \cdot 10^5$ N/m^2 (saturated steam)

p_4 = 2.55 psia = $0.175 \cdot 10^5$ N/m^2

Maximum Mach Number is $\sim$ 0.75.

The test section is located after a stilling tank which is supplied with low pressure steam from the laboratory heating supply ($\sim$5 psig, 0.9 quality). A diffuser then guides the steam to a jet-cooled condenser. The test section is of plexiglas , so that the liquid droplets downstream, as well as th liquid film upon the inserted flat plate, can be easily observed This plate, which replaces a turbine fixed blade, is located inside the test section (Fig. 2). A thin liquid film was obtained upon the blade by means of a slot placed near the leading edge (Fig. 3). Water flow-rate was measured by a flow meter, and liquid film thickness by means of the residence

gage method (5), (6), using four gages in the plate surface. The flow rate and liquid film thickness were as follows:

$$\dot{q} = 2.5 \sim 10 \text{ cm}^3/(\text{cm} \cdot \text{min})$$
$$h = 50 \sim 250 \ \mu\text{m}$$

The liquid film on the plate appeared first to disintegrate into liquid filaments, and next into "secondary" droplets (Fig. 4). These then pass downstream in the aerodynamic wake, still being disintegrated due to the increasing aerodynamic forces, since the velocity of the wake increases with distance downstream from the trailing edge.

This liquid-phase behavior was studied photographically. The camera was located as close as possible to the test section, producing a magnification of $\sim$2.4x. A light flash duration of $\sim$ 1 us has been used, with light source perpendicular to camera axis (Fig. 2). This was most suitable, as pictures so taken were sharp and with good contrast. Several typical pictures are included in this report (Fig. 4-9). Droplet size measurement capability was, however, limited to droplets above $\sim$ 50 μm diameter because of limited optical resolution of the camera and film. Smaller droplets had too great velocity to be recorded with the available flash duration. These limitations proved most significant at high Mach number (M $\sim$ 0.75), and relatively long distances downstream of trailing edge.

We hope to develop another method for small droplets well downstream and at high Mach number. This method will be based

on laser light scattering from small particles, and should be useful for the measurement of 1 $\sim$ 20 μm droplets.

RESULTS OF THE EXPERIMENT

Because of the erosion threat to turbine blading, informatio of maximum droplet size is important. Many photographs ($\sim$ 300) have been made at three Mach numbers;

$$M = 0.35;\ 0.55;\ 0.75$$

and at three values of the flow rate:

$$\dot{q} = 2.5;\ 5.0;\ 10.0 \quad cm^3/(cm \cdot min).$$

Several relationships have been obtained. These are presented in Fig. 10-12. All large droplets provide data points on these graphs according to their distance downstream in aerodynamic wake (x-coordinate). The relationship between maximum droplet size and distance downstream, $D_{max} = f(x)$, is established as a limiting line above the area of the data points. This function has been shown as a belt because the process of liquid phase disintegration is very non-uniform.

The function $D_{max} = f(x)$ decreases with distance x until $x \simeq 20$ cm and then remains essentially constant. It is independent of liquid flow rate for this experiment. However, the shape of the curves depends very strongly on the Mach number (Fig. 13).

To allow application of these results for other conditions, a more universal relationship has been generated. Using the results of Fig. 13, and transforming them into a dimensionless function of Weber number,

$$We_{max} = f\ (M),$$

the relationship of Fig. 14 was obtained. Here

$$We_{max} = \frac{\varrho \cdot V_\infty^2 \cdot D_{max}}{\sigma}$$

D_{max} = maximum droplet size, from center of data scatter, at distance x = 22 cm, assuming maximum droplet size to be approximately constant for distances longer than x = 22 cm

V_∞ = the velocity of the steam outside of the aerodynamic value

Results obtained by other authors are also presented, i.e., Weigle and Severin (7), using an air tunnel, and Valha from a steam tunnel (8).

To obtain further information on liquid droplet stream structure, still another approach was applied. Based on several droplet pictures (Fig. 4-9), a droplet size distribution function has been established.

This function is defined as follows:

$$F(d) = \frac{N(d)}{N} \cdot \frac{1}{\Delta d}$$

where:

d = droplet size

Δd = droplet size interval (Δd = 200 μm for presented experiment)

N(d) = average number of droplets of the size enclosed in the region $(d - \frac{\Delta d}{2}, d + \frac{\Delta d}{2})$,

N = average total number of the droplets visible in the test area.

In order to obtain the above function, droplets visible on the picture were counted according to their sizes (using a magnifying glass with scale). Consequently, the droplet size distribution

function was used to establish a droplet mass distribution function:

$$R(m) = \frac{m(d)}{m}\frac{1}{\Delta d} = \frac{d_i^3 \cdot N(d_i)}{\sum_{i=1}^{i=n} d_i^3 N(d_i)}\frac{1}{\Delta d} = \frac{d_i^3 F(d_i)}{\sum_{i=1}^{i=n} d_i^3 F(d_i)}\frac{1}{\Delta d}$$

where:

$m(d)$ = average mass of droplets of the size enclosed in the region $(d - \frac{\Delta d}{2}, d + \frac{\Delta d}{2})$

m = average total mass of the droplets visible in the test area.

$$n = \frac{d_{max}}{\Delta d}$$

Both functions were normalized in order that the integral is equal to one.

The results of the experiment reduced to size and mass distribution functions are shown on Figs. 15-18 for the following values of the Mach number:

$M = 0.35$

$M = 0.55$ *

To be sure, both functions are being changed according to the distance x; the ratio of large droplets decreases, and the ratio of small droplets increases. The same effect takes place as Mach number increases. The highest probability of droplets occurring (the maximum of the function of probability density) is shown below in the conclusions.

*Unfortunately it was impossible to obtain any droplet size mass distribution function at $M_a = 0.75$. The cause has been discussed above. The same difficulty appeared for long distances (x) between the trailing edge and the test area.

CONCLUSIONS

1. The maximum droplet size function $D_{max} = g(x,M)$, decreases with the distance x and Mach number M . D_{max} becomes constant for distance $x \geq 22$ cm. In this region, maximum droplet size varies with Mach number.

$M = 0.35;\quad D_{max} = 750\ \mu m$
$0.55;\quad 500\ \mu m$
$0.75;\quad 250\ \mu m$

The variation of D_{max} with respect to x and M proved to be different than had been estimated theoretically based on the steam velocity distribution in the aerodynamic wake and assumed critical Weber number, (We = 13) (1). Droplet diameter here measured is at least twice that estimated before.

2. The critical value of the Weber number

$$We = \frac{\rho \cdot V_\infty^2 D_{max}}{\sigma}$$

has been estimated as follows:

$M = 0.35 \quad We \cong 30$
$M = 0.5;\ 0.75; \quad We \cong 45 \qquad$ (Fig. 14)

3. The most probable droplet size to appear in the aerodynamic wake, in the vicinity of the trailing edge (x = 2.5 to 4 mm), according to the size distribution function is:

$M = 0.35; \quad d \cong 250\ \mu m$
$M = 0.55; \quad d \cong 133\ "$

and according to the mass distribution function:

$M = 0.35; \quad d \cong 500\ \mu m$
$M = 0.55; \quad d \cong 475\ "$

4. There is no significant influence of (water) liquid film flow rate (up to $\dot{q} = 10\ cm^3/cm.s$) on the maximum droplet size D_{max}, and on the droplet size and mass distribution function F(d), R(m).

REFERENCES

1. Puzyrewski, R. and Krzeczkowski, S., "Some Results of Investigations on Water-Film Break-Up and Motion of Water Drops in Aerodynamic Trail," IFFM Trans., 29-31, 1966, Gdansk, Poland.
2. Christie, D. G., and Haywood, G. W., "Observation of Events Leading to the Formation of Water Drops Which Cause Turbine Blade Erosion," Phil. Trans. Roy Soc., 260 SA, No.1 London, 1966.
3. J. P. Faddeev, Proceedings of the III Conference on Steam Turbine of Great Output, Prace IMP-PAN, Gdansk, Poland, 197
4. Krzyzanowski, J., "Wet-Steam Tunnel Facility-Design and Program of Investigations", ORA Report No. UMICH 03371-18-T, Univ. of Mich, Ann Arbor, Mich., 1972.
5. Puzyrewski, R. and Jasinski, R., "Measurement of the Thickn of Thin Water Films by Resistance Method," IFFM - Trans. No 1965, Gdansk, Poland.
6. Mikielewicz, J., Hammitt, F. G., "Generalized Characteristi of Electrical Conductance Film Thickness Gauges," Proc. 6th Steam Turbines Large Output, Pilsen, Czech. 16-19, Sept. 19

ACKNOWLEDGMENTS

The financial support of this investigation is provided by National Science Foundation Grants No. ENG 75-2315 and GK-40130. The authors are indebted to Professor Jerzy Krzyżanowski, Instit of Fluid Machinery, Polish Academy of Science, Gdansk, for the preliminary design of the facility and constant helpful suggesti

List of Figures

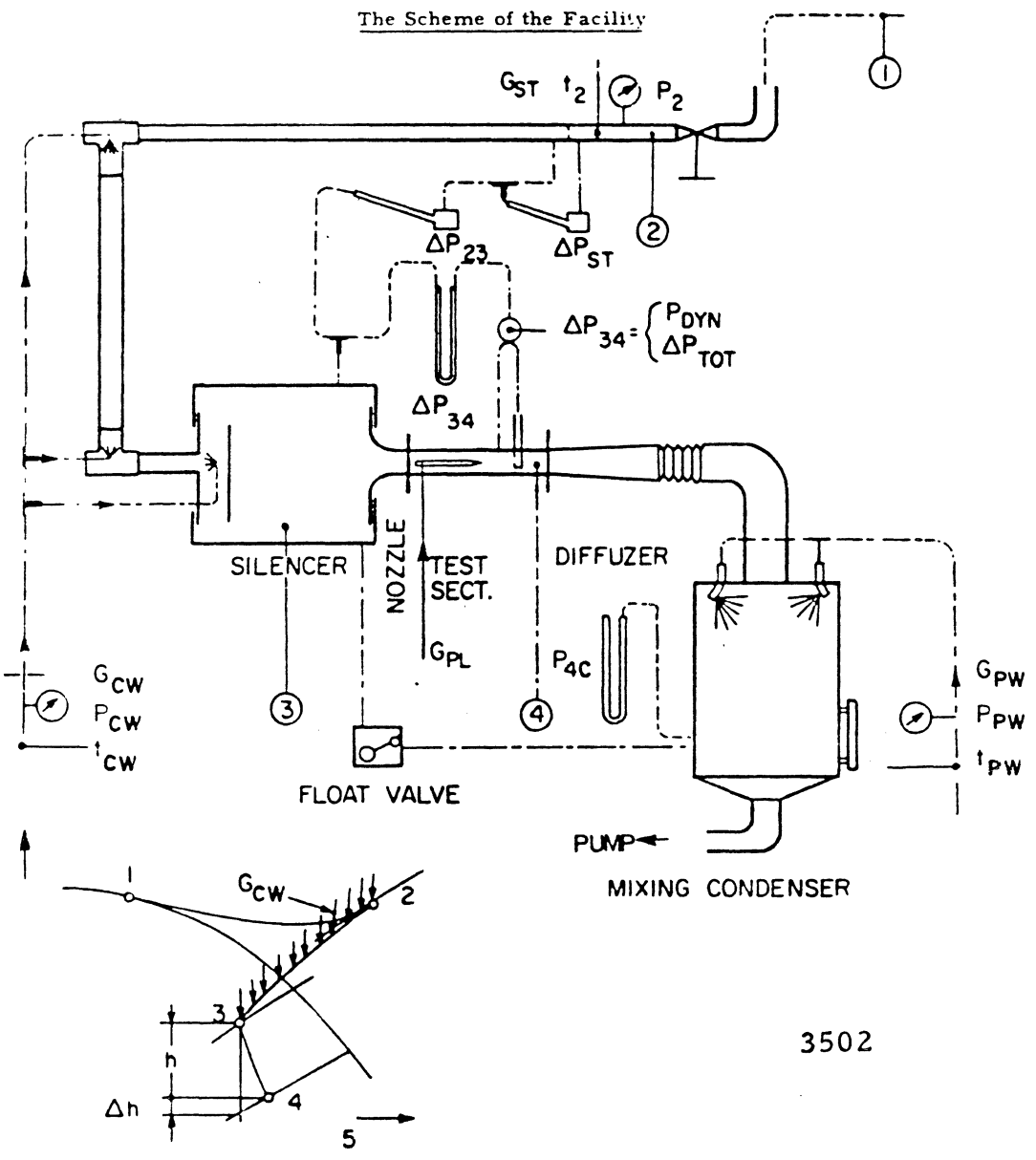

Figure 1 - Schematic Diagram of the University of Michigan Steam Tunnel (4)

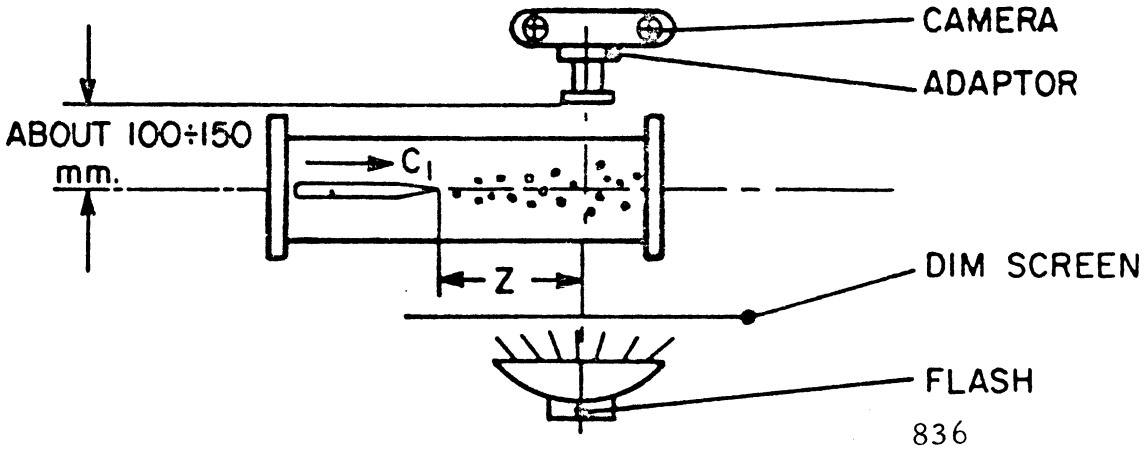

Figure 2 - Schematic of Test Section and the Position of Camera and Flash (4)

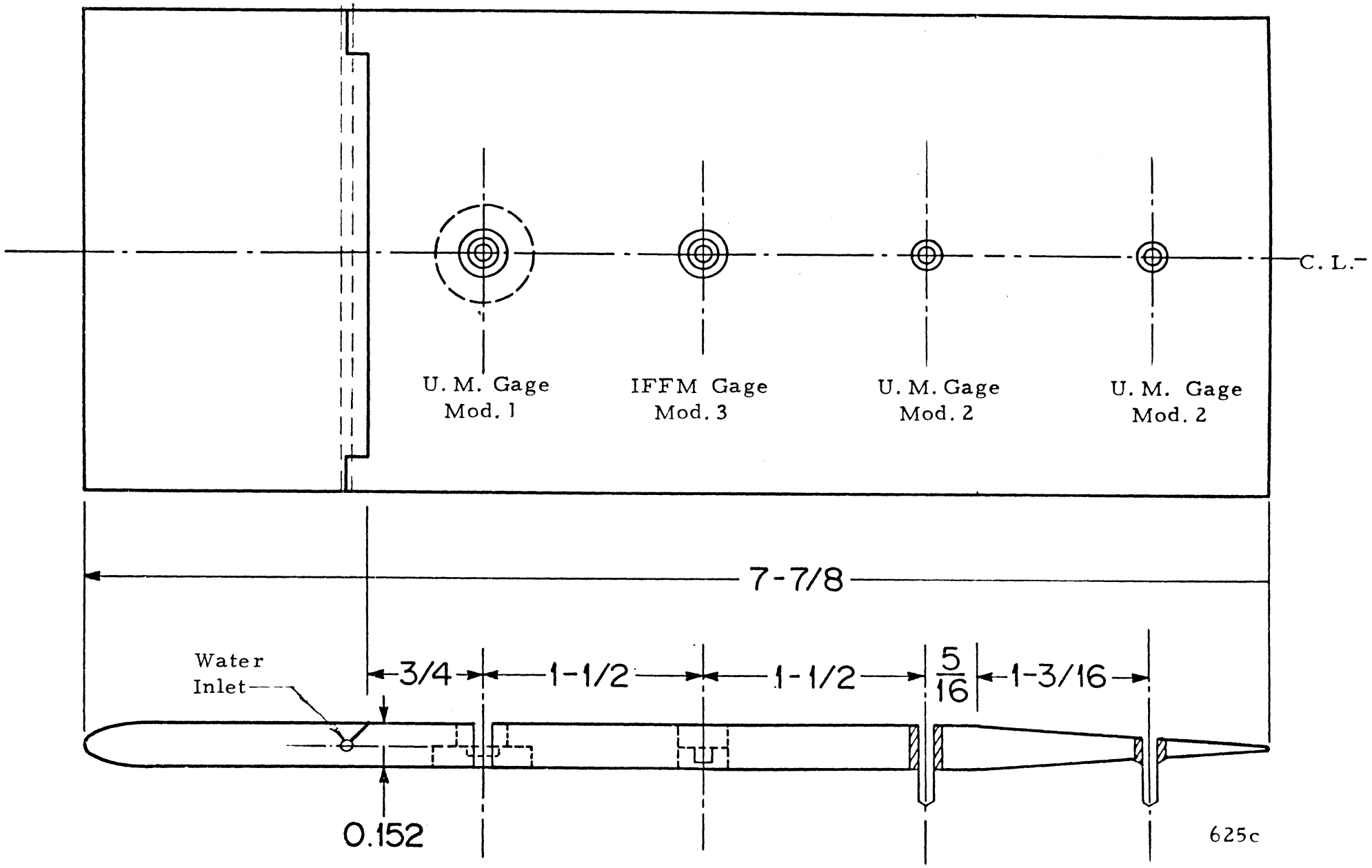

Figure 3 - Schematic of Blade with Gases

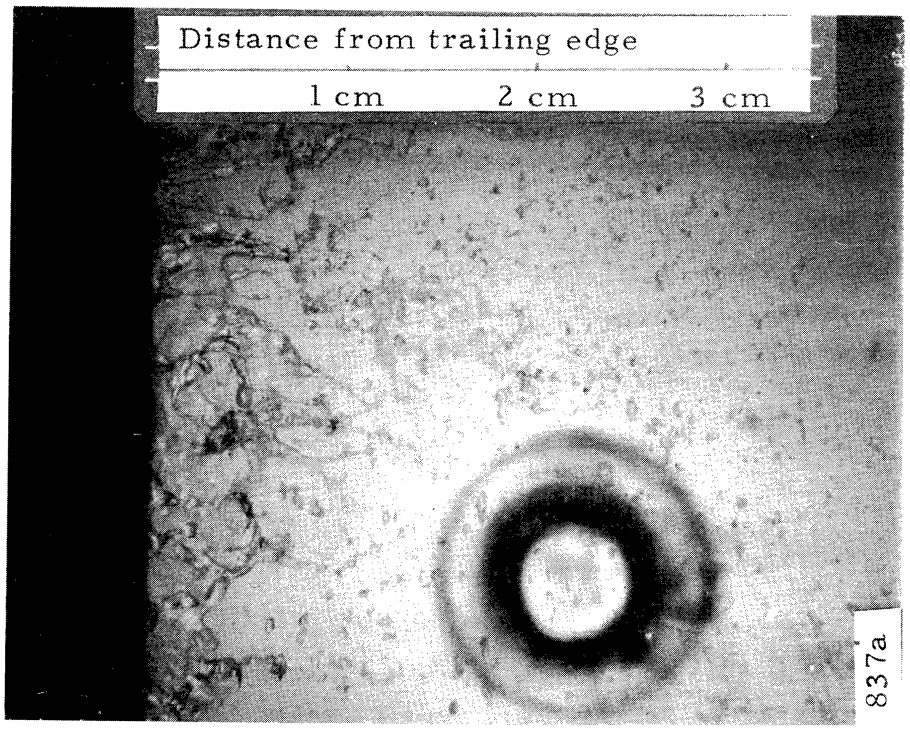

Figure 4 - Photographs of Liquid Film Disintegration into Droplets at the Trailing Edge, M = 0.35, $\dot{q}$ = 5 $cm^3/cm \cdot min$.

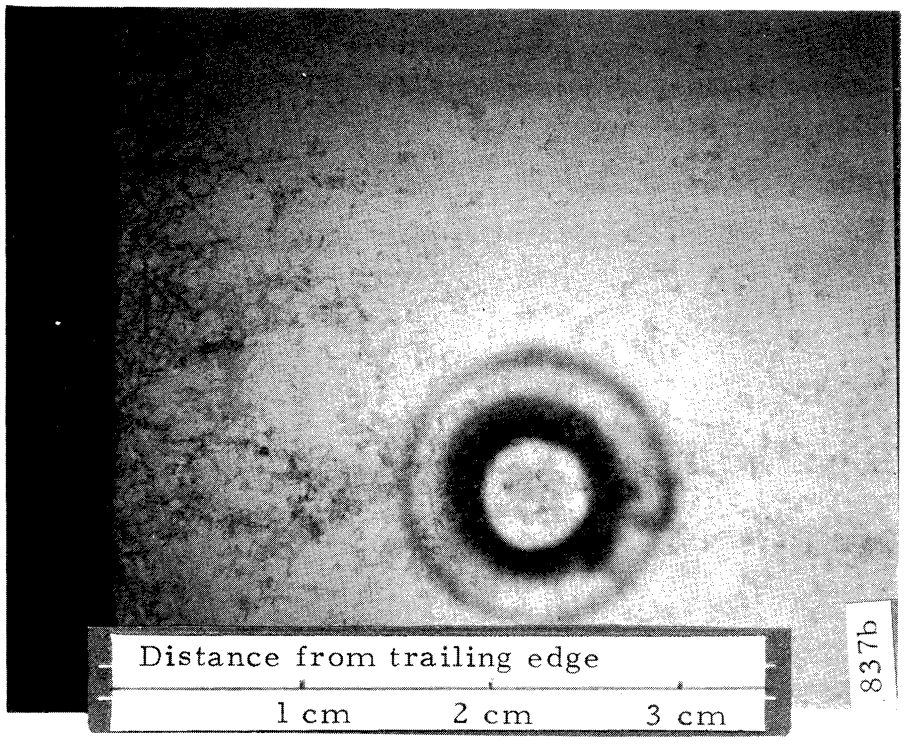

Figure 5 - Photographs of Liquid Film Disintegration into Droplets at the Trailing Edge, M = 0.55, q. = 25 $cm^3/cm \cdot min$.

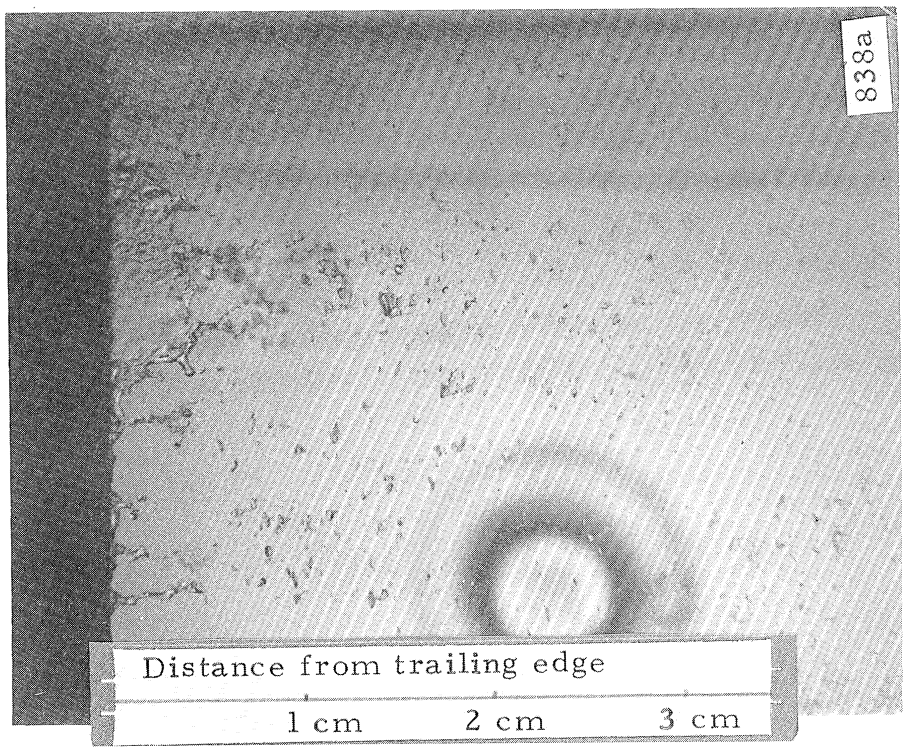

Figure 6 - Photographs of Liquid Film Disintegration into Droplets at the Trailing Edge, M = 0.75, q_o = 5 $cm^3/cm \cdot min.$

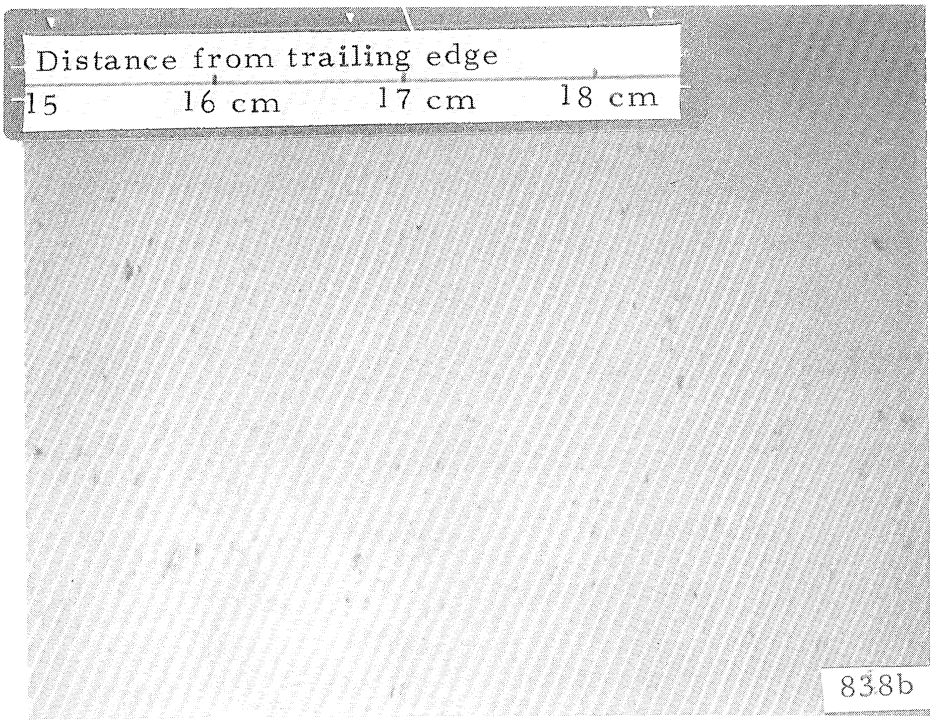

Figure 7 - Photographs of Liquid Droplets Distribution in Downstream Flow, M = 0.35, q = 10 $cm^3/cm \cdot min.$, X = 14 cm

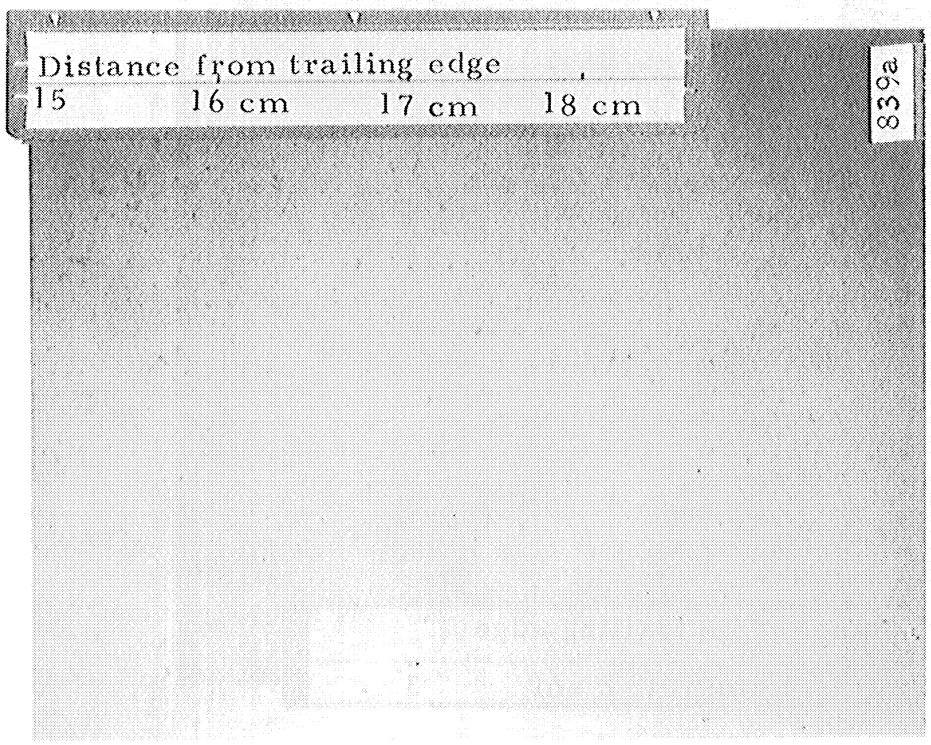

Figure 8 - Photographs of Liquid Droplets Distribution in Downstream Flow, M = 0.55, q = 10 $cm^3/cm \cdot min$. X = 14 cm

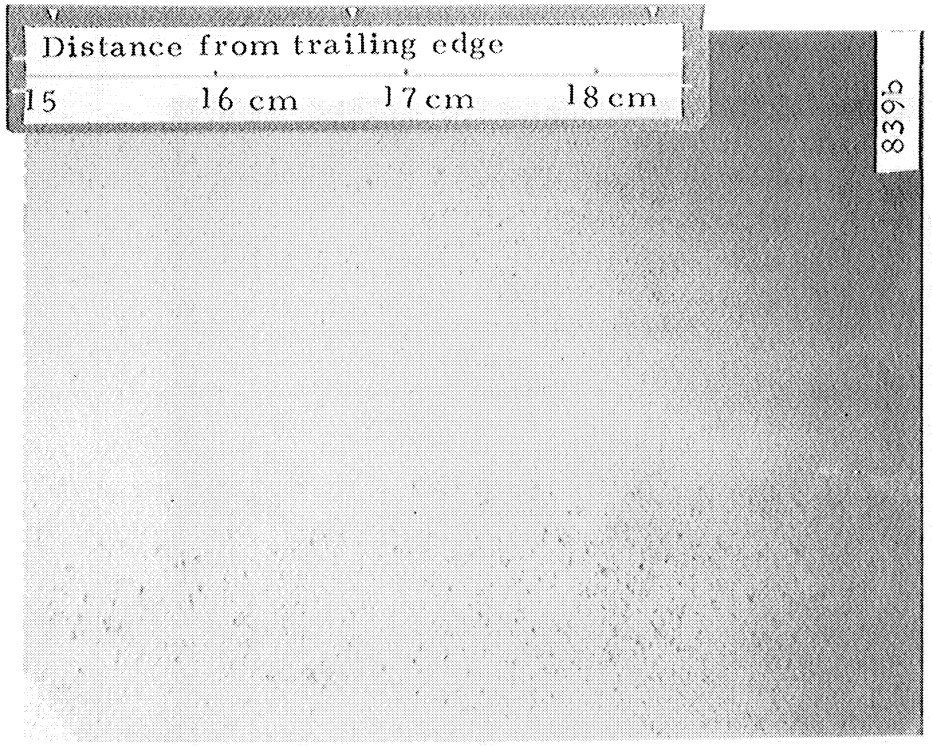

Figure 9 - Photographs of Liquid Droplets Distribution in Downstream Flow, M = 0.75, q = 10 $cm^3/cm \cdot min$. X = 5 cm

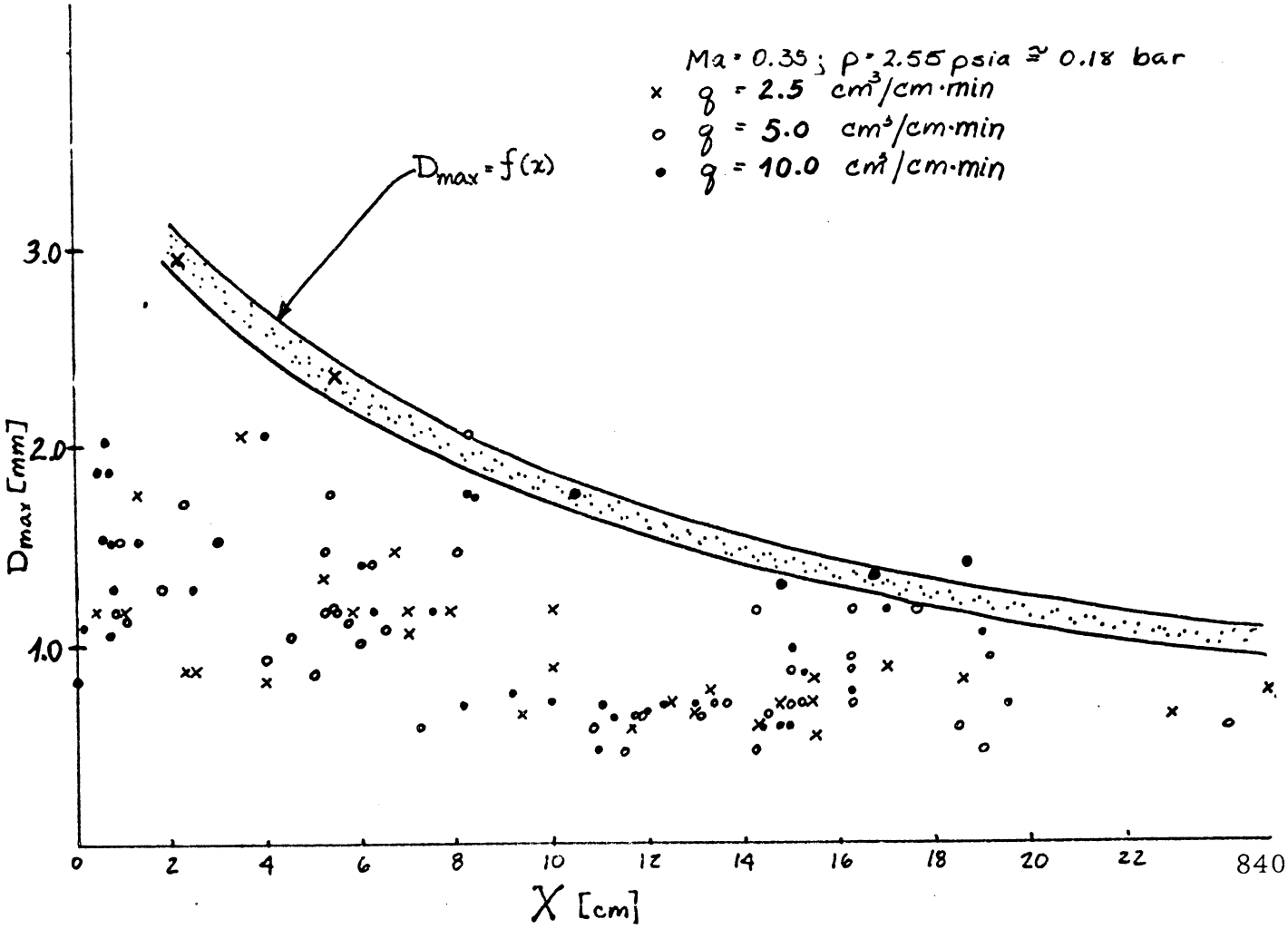

Figure 10 - Maximum Droplet Size as a Function of the Distance From the Trailing Edge, M = 0.35

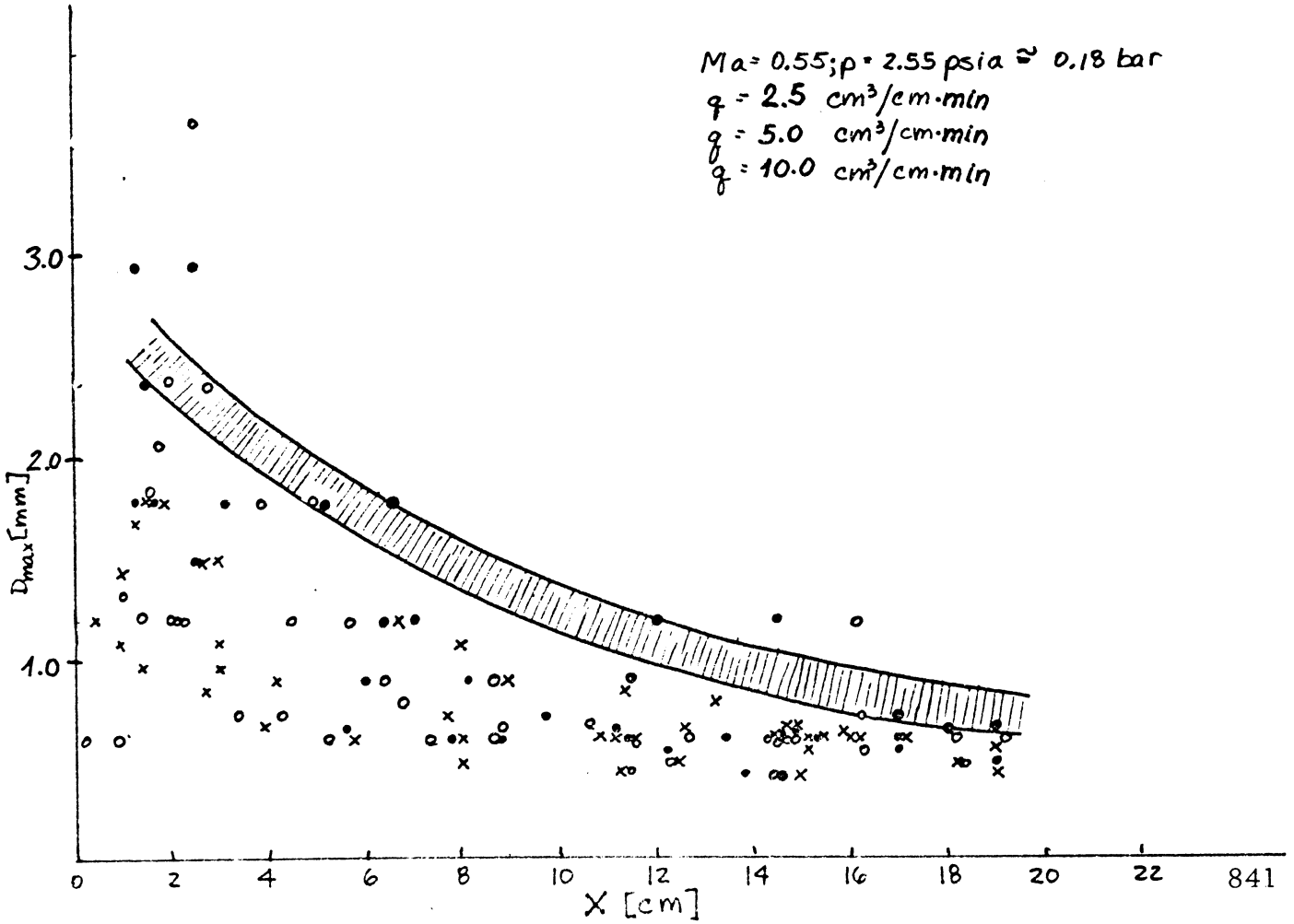

Figure 11 - Maximum Droplet Size as a Function of the Distance From the Trailing Edge, M = 0.55

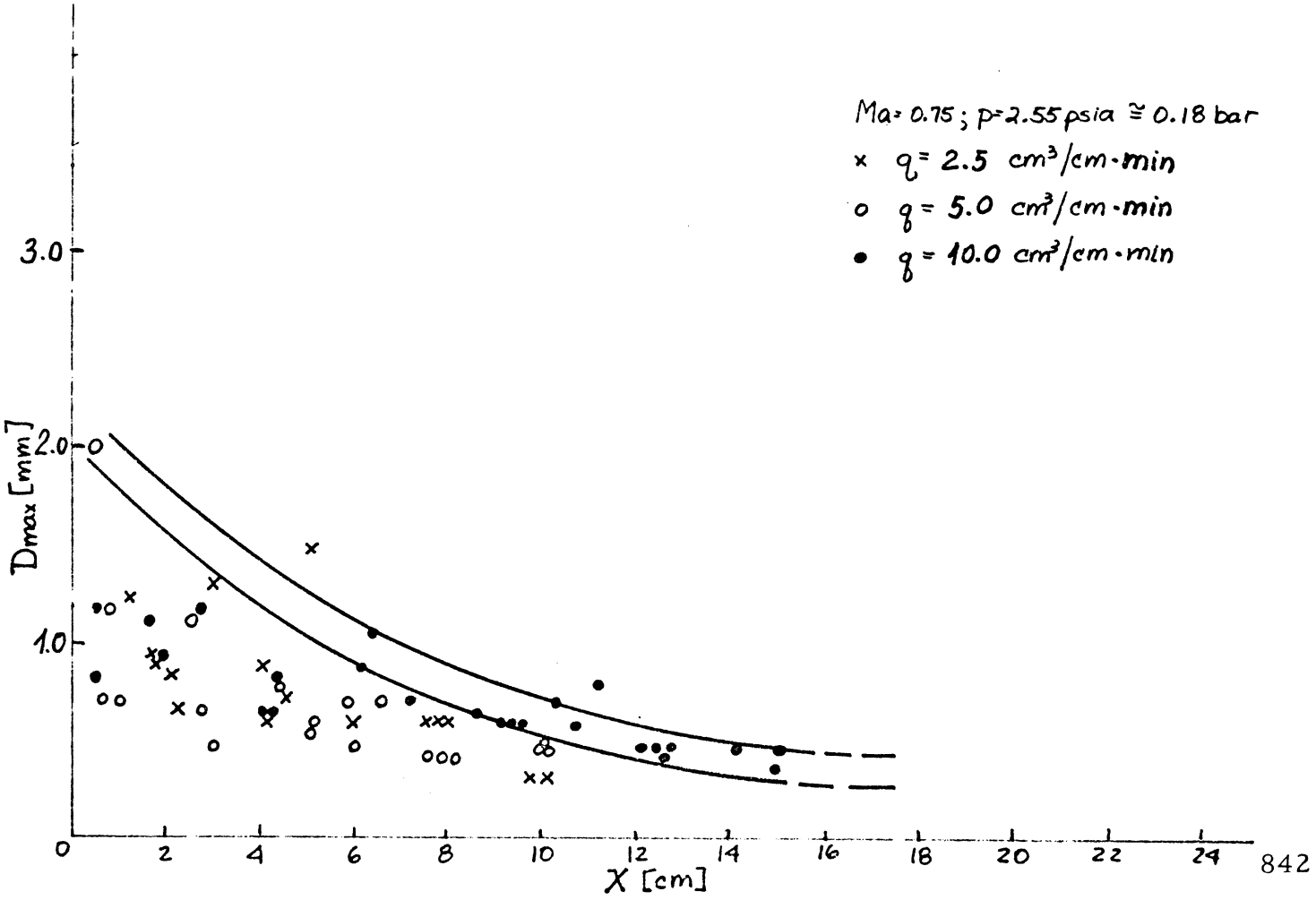

Figure 12 - Maximum Droplet Size as a Function of the Distance From the Trailing Edge, M = 0.75

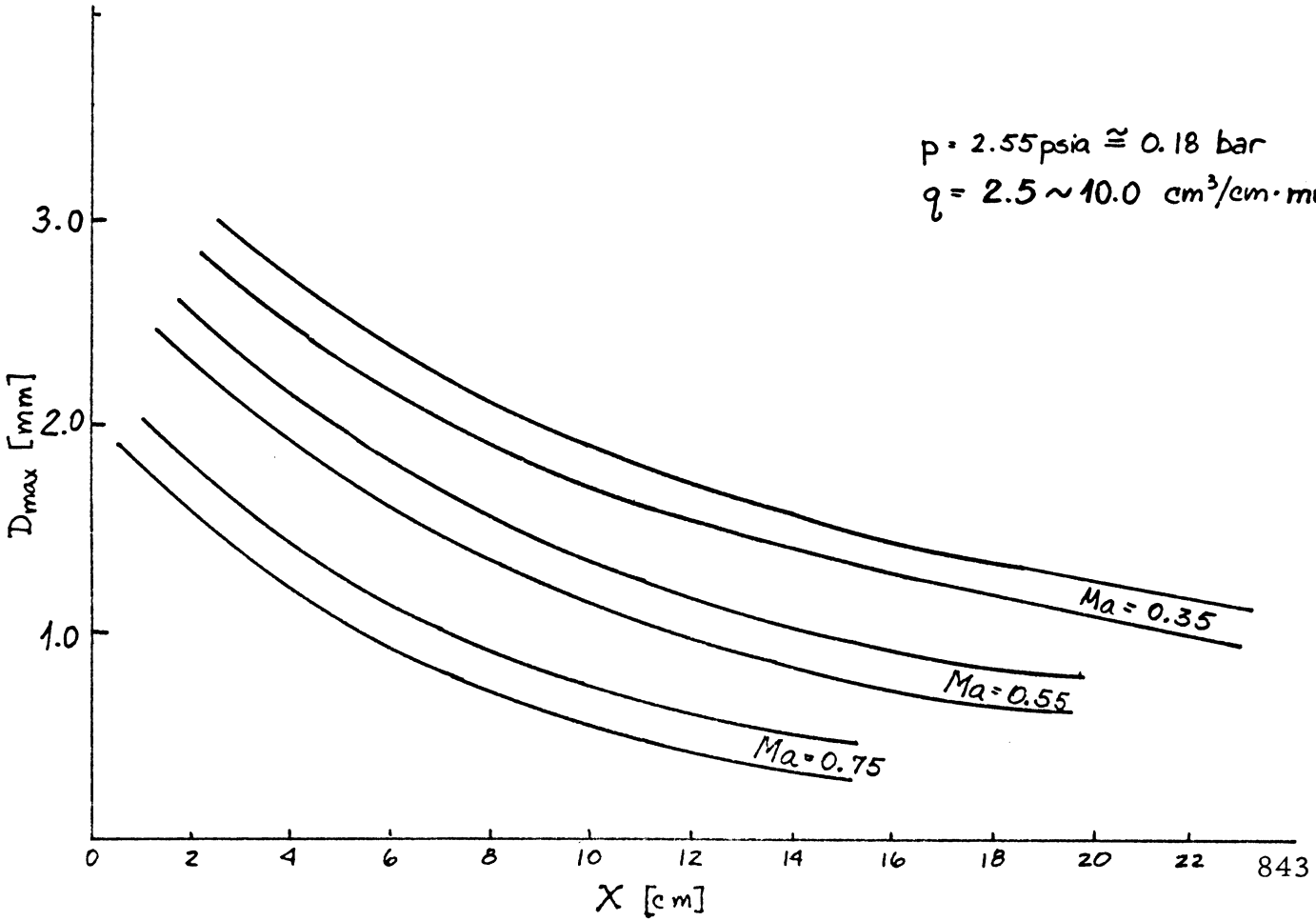

Figure 13 - Maximum Droplet Size as a Function of the Distance From the Trailing Edge at three Mach Numbers

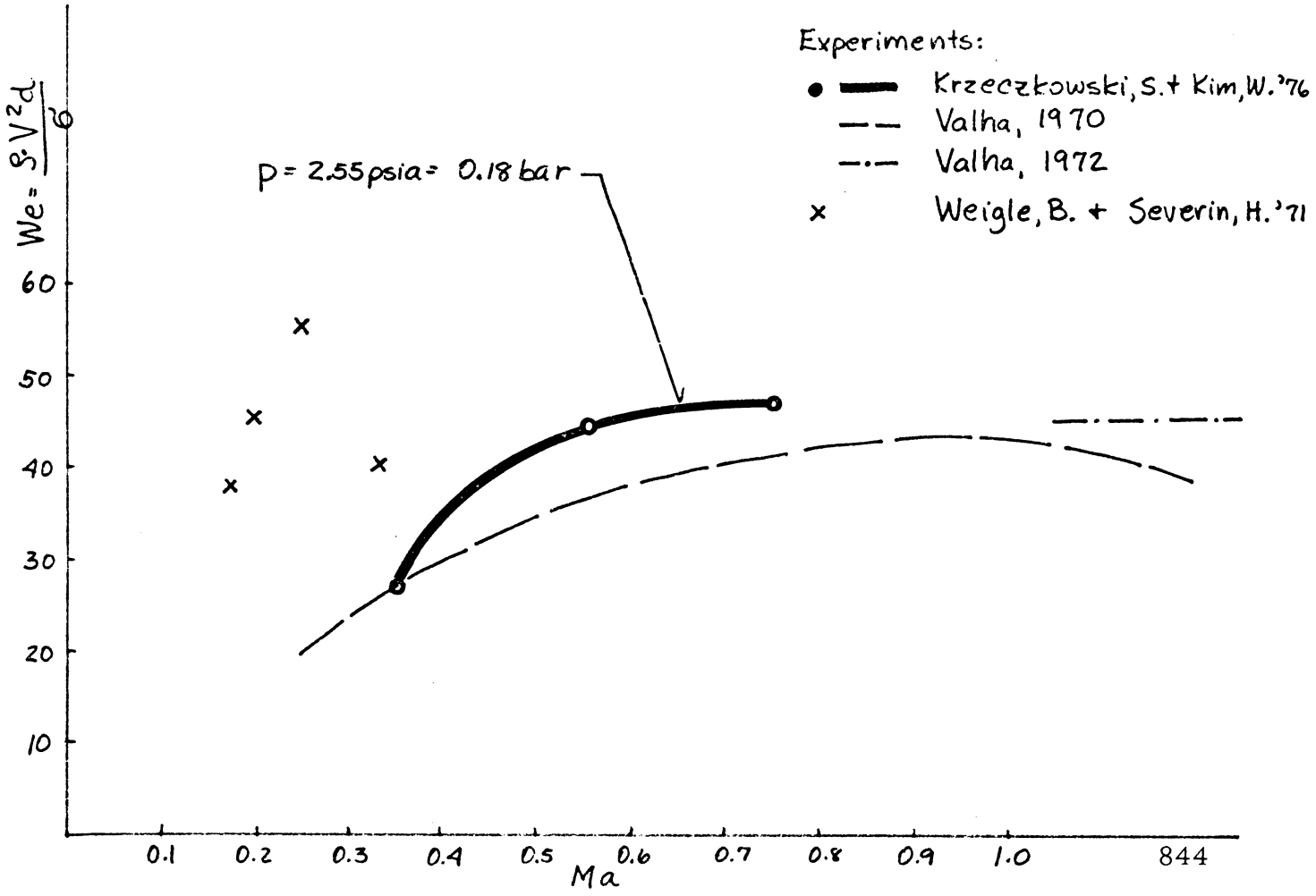

Figure 14 - The Weber Number of Maximum Droplets for Downstream From the Trailing Edge

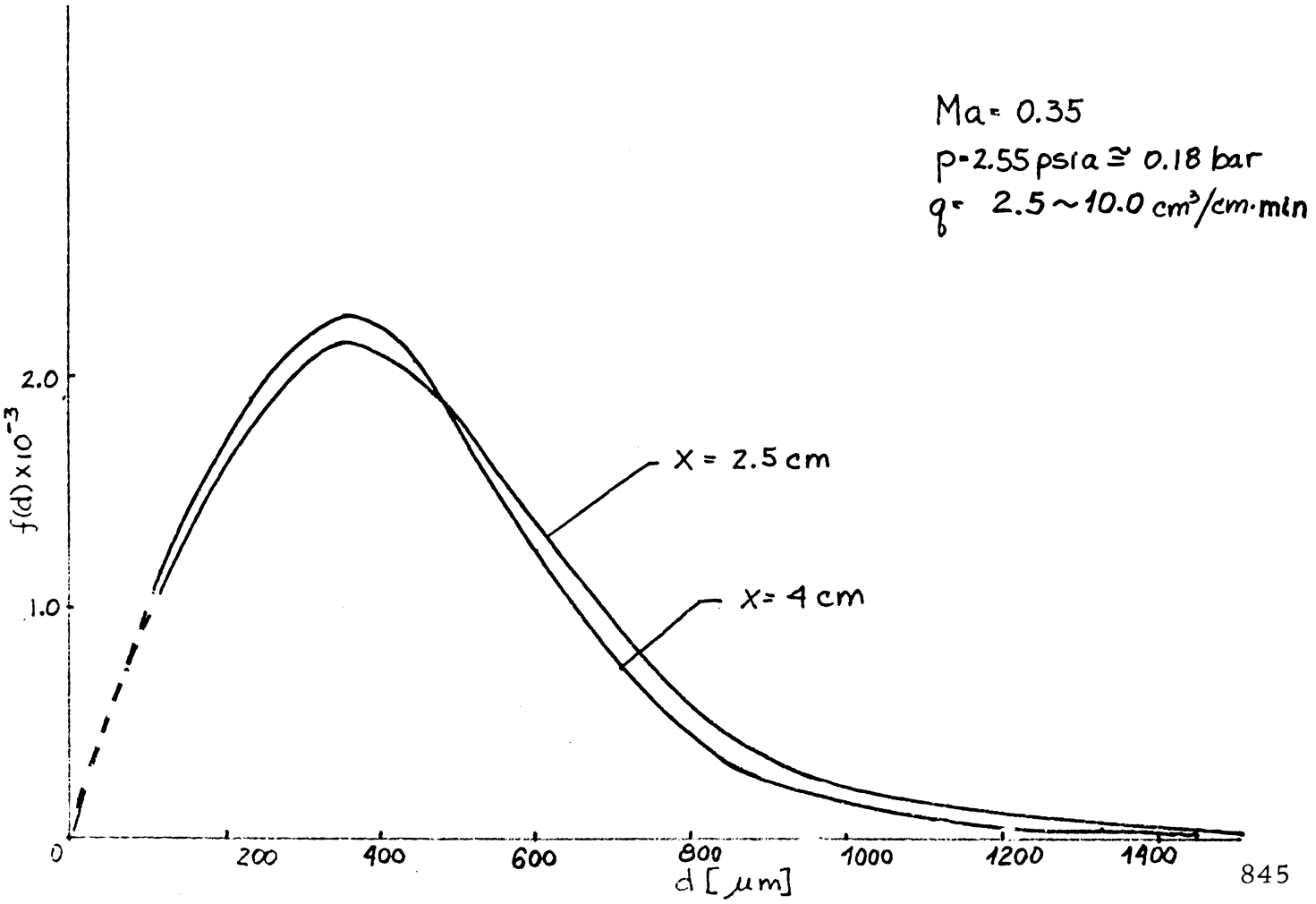

Figure 15 - Droplet Size Distribution Function at M = 0.35, X = 2.5 cm and X = 4.0 cm.

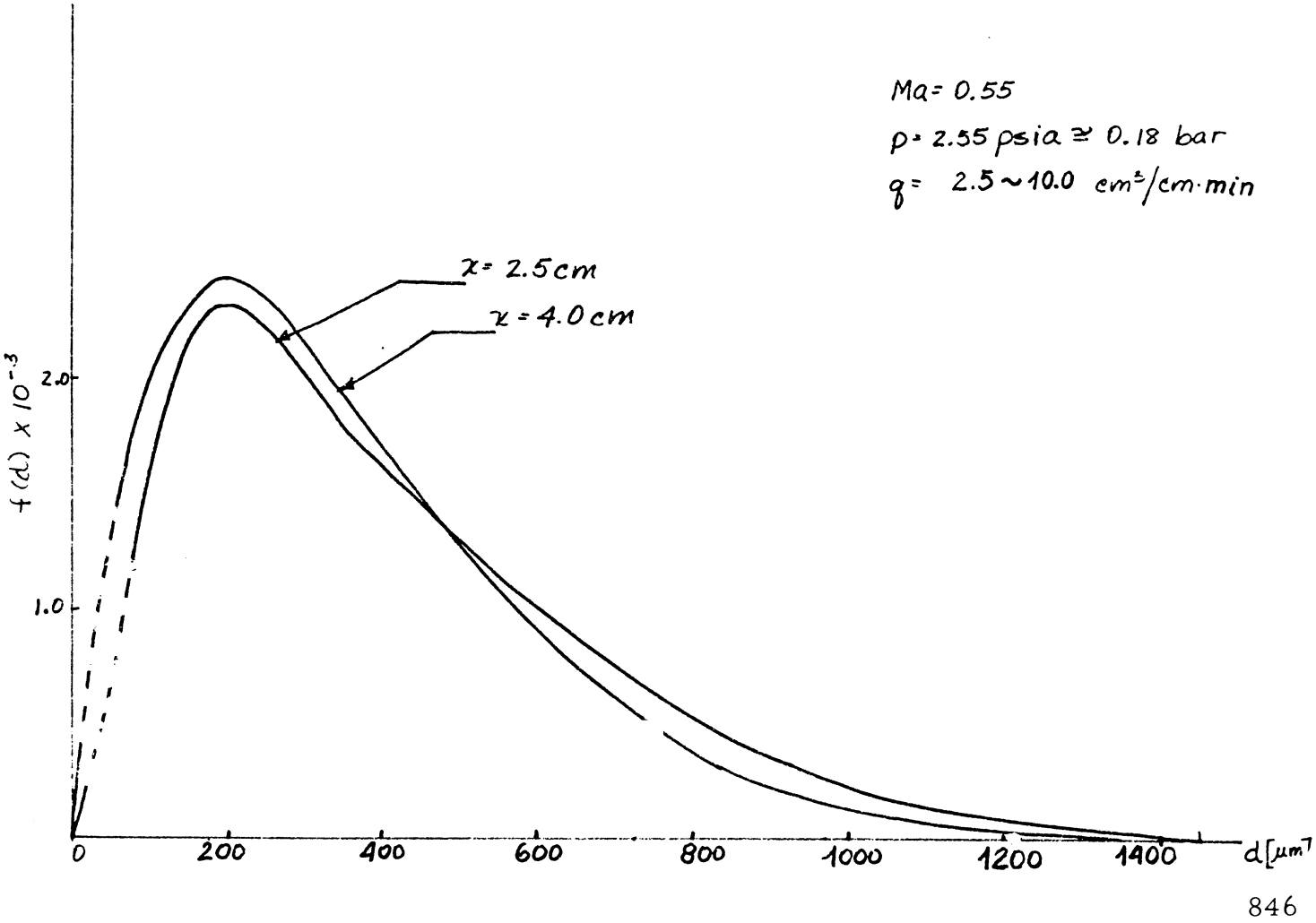

Figure 16 - Droplet Size Distribution Function at M = 0.55, X = 2.5 cm and X = 4.0 cm.

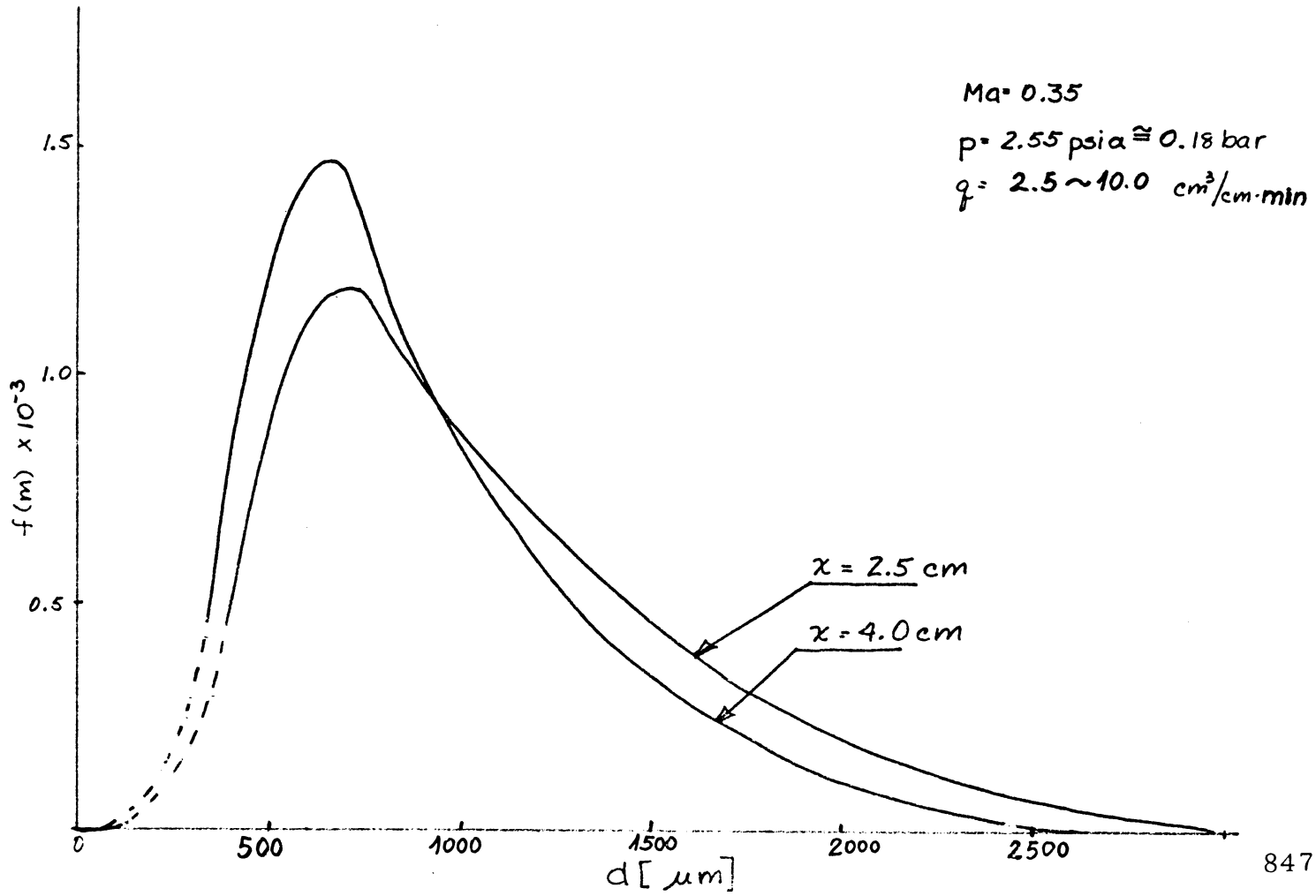

Figure 17 - Droplet Mass Distribution Function at M = 0.35, X = 2.5 cm and X = 4.0 cm

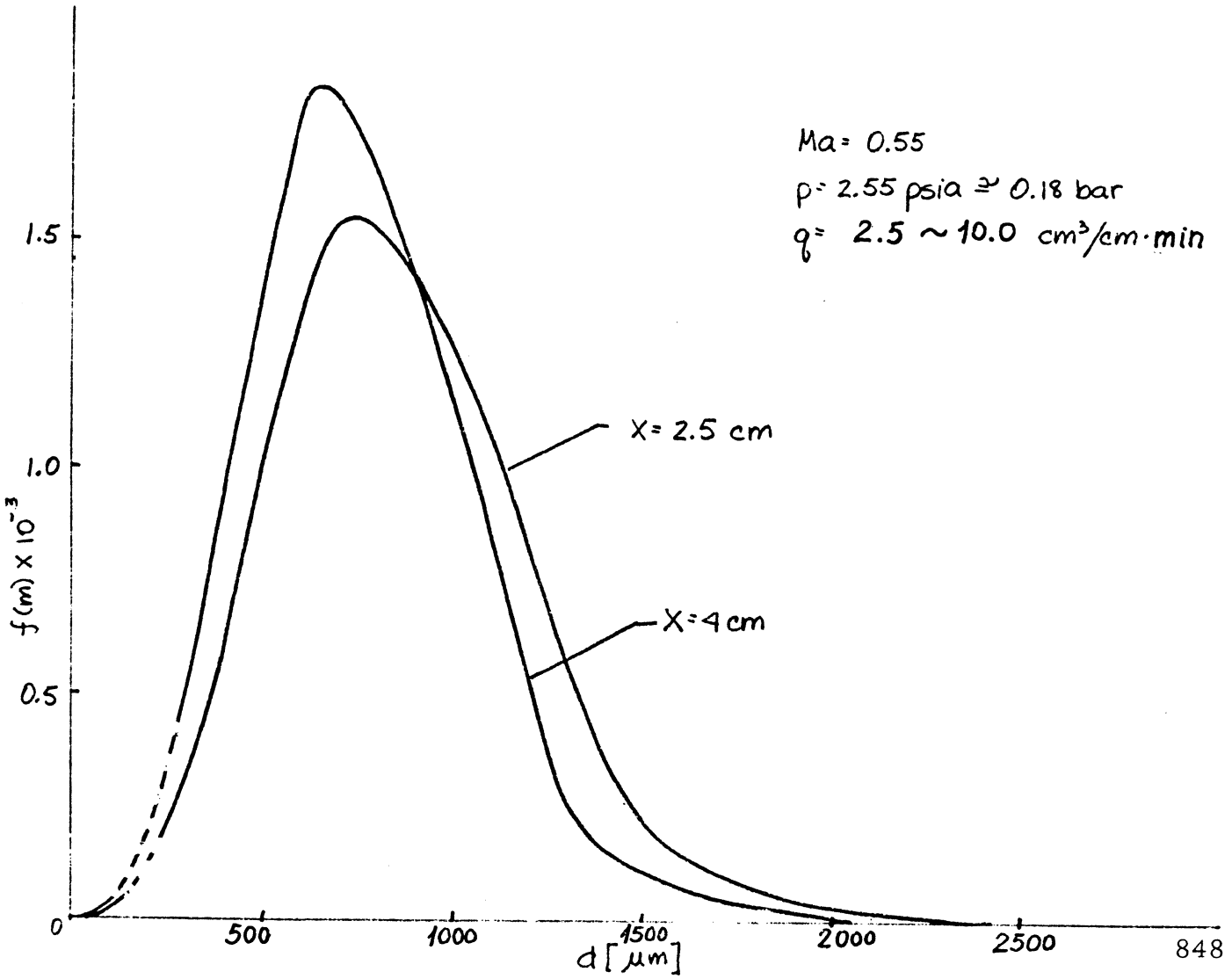

Figure 18 - Droplet Mass Distribution Function at M = 0.55, X = 2.5 cm and X = 4.0 cm.